General Disclaimer

One or more of the Following Statements may affect this Document

- This document has been reproduced from the best copy furnished by the organizational source. It is being released in the interest of making available as much information as possible.

- This document may contain data, which exceeds the sheet parameters. It was furnished in this condition by the organizational source and is the best copy available.

- This document may contain tone-on-tone or color graphs, charts and/or pictures, which have been reproduced in black and white.

- This document is paginated as submitted by the original source.

- Portions of this document are not fully legible due to the historical nature of some of the material. However, it is the best reproduction available from the original submission.

Produced by the NASA Center for Aerospace Information (CASI)

RESEARCH

ENGINEERING

ENGINEERING

RESEARCH

ENGINEERING

RESEARCH

ENGINEERING

RESEARCH

INSTITUTE

IOWA STATE

UNIVERSITY

AMES, IOWA

ENGINEERING

RESEARCH

ENGINEERING
RESEARCH
ENGINEERING
RESEARCH
ENGINEERING
RESEARCH
ENGINEERING
RESEARCH
ENGINEERING
RESEARCH

FINAL REPORT
LOAD DEFLECTION CHARACTERISTICS
OF INFLATED STRUCTURES

JOSEPH R. BAUMGARTEN
OCTOBER 1983

i

TABLE OF CONTENTS

1. PROLOGUE

This research, funded by NASA Grant NSG 1605, was initiated April 1, 1979 by the Principal Investigator Joseph R. Baumgarten at the Iowa State University, Department of Mechanical Engineering. Over the duration of this grant, from April 1, 1979 to November 30, 1983, seven graduate dissertations have been written from investigations conducted in conjunction with this work. Two refereed papers in the technical literature have resulted to date directly from this particular grant; three more papers are anticipated.

This present grant, NSG 1605, has been a continuation of work initiated by the principal investigator, and funded by NASA, while he was a member of the faculty of the University of Nebraska. The initial NASA Grant NSG 1506 was concerned with air springs and began with the study of load-deflection characteristics of an inflated torus with inelastic walls. The desire to include wall elasticity in the analysis of inflated structures has prompted this present work.

2. INTRODUCTION

Many examples of the employment of inflated structures in load bearing applications can be found. Vibration isolation of heavy machinery is best achieved by use of air springs. One popular commercial type of air spring consists of a spherical rubber wall vulcanized to top and bottom steel plates. Some air spring designs consist of a piston displacing in a rigid wall steel cylinder. In either case, the load deflection characteristics for the physical system are needed if the resulting natural frequency of the mounted machine is to be known. Earlier work by the Principal Investigator with colleagues Orley [1,2][*] and Andersen [3,4] indicated that air springs did not show a simple linear volume-natural frequency relationship. As volume was quadrupled, spring rate was not quartered and, hence, natural frequency was not halved. A closed form relation resulted from Andersen's work [3] which would predict the deflection of the horizontal torus at a given load. This derivation assumed inelastic walls and gave excellent results for predicted spring rates in low ranges of torus deflection (up to 10% of undeflected height).

The investigation by Chomos [5] was the initial effort to include wall elasticity in the load-deflection analysis of an inflated torus. This work was supported by NASA-Langley Research Center under Grant NSG 1506. The analytical results of Chomos were checked by finite difference-finite element numerical procedures (using STAGS1) by the principal investigator [5].

Chomos' work resulted in three simultaneous equations which required

_____

[*] Numbers in brackets indicate references.

a computer based iterative technique to find the analytical solution for the compressed torus dimensions at a given load. The work initiated under the current contract, NASA Grant NSG 1605, sought a single closed form solution to relate load to deflected torus dimensions for the horizontal torus. Oguoma [6], attributed the initial study of a horizontal torus with elastic walls at Iowa State University.

Research has been underway to define the response of air cushion landing systems for conventional aircraft. The load bearing structure in this case is an inflated cushion made of fiber reinforced laminate. If load-deflection characteristics were known for these ellipsoids and toroidal structures, dynamic response of the landing system could be better analyzed. Analysis has been completed of toroidal inflated Mars Landers. The devices consist of a platform mounted centrally in an inelastic rubber reinforced fiber torus. The loading is along an inner peripheral ring.

An inflated aircraft tire constitutes a third class of structure of interest to this present grant. This toroidal body (a standing torus) must deform and restore several times in the landing cycle. All braking, cornering, and rolling maneuvers must be accomplished thru the tires. It is highly desirable in this case, also, to predict the dynamic response of the system.

This third class of inflated structure, the standing torus, has been the major interest in the present study (NASA Grant NSG 1605). Gassman [7] contributed equations relating vertical load to torus deflection and footprint area. Mack [8] studied the standing torus analytically, using a revised finite element computer technique, STAGSC, to compare analysis with Gassman's results. Hill [9] used mercury strain gages to produce

experimental strain readings of the standing torus. Miller [10] studied the standing torus under combined vertical and braking loads by use of the revised STAGSC1 computer program. Bucher [11] studied boundary conditions of the loaded torus at the rim by use of STAGSC1. His studies gave improved agreement with the strain measurements of Hill. Tau [12] studied the standing torus under combined vertical and cornering loads by use of the STAGSC1 finite element computer algorithm.

In September 1982, the Principal Investigator was granted a leave of absence in order to join the faculty of Afdeling Werktuigboukundig, Technische Hogeschool, Delft, The Netherlands for one year. Donald R. Flugrad, Assistant Professor of Mechanical Engineering, Iowa State University joined the NASA project at that time and worked closely with Mr. Miller and Mr. Pau as research advisor and Co-Principal Investigator. Flugrad was especially active in the investigations of combined normal and braking load analysis and combined normal and cornering load analysis. His insight and advice helped define the basis for the determination of contact area from force-deflection iteration schemes.

3. LOAD-DEFLECTION ANALYSIS OF A HORIZONTAL TORUS

Oguoma [6] initiated work under the present contract, NSG 1605, in his study of a horizontal torus loaded by a plane. The initial thrust of this work consisted of developing a single, closed-form relationship to relate load to the deformed dimensions of the horizontal torus. Wall elasticity was included in the analysis, and special care was taken to predict the final footprint area of the loaded structure.

The test fixture utilized in this study is shown in Figure 1. The equipment utilized in the course of this research was by no means complicated or exotic. The tori used for the bulk of the testing were rubber inner tubes for a 4.00 x 8 and an 8.00 x 20 pneumatic tire. The inner tube being tested was plumbed to a mercury-filled manometer, which had a 50 inch measurement capacity, by use of a special adapter. The adapter fit over the valve stem and allowed air to be added from a shop-air source and to be bled thru the standard valve mechanism. In this fashion, tests requiring the maintenance of a constant indication of air pressure could be run with little difficulty. All connections at the adapter and throughout the pressure line were well sealed with rubber cement.

Two flat surfaces were used to compress the torus. Both planes were made from 3/4 inch plywood. The bottom flat included a hole large enough to allow measurement of the inner diameter of the tube with an inside caliper. In order to maintain parallel surfaces between planes as load was applied, a swing or load platform was suspended from the upper plane thru the torus and bottom plane as Figure 2 illustrates. Weights were applied to the platform and a single vertical load vector resulted on the upper plane. In order to measure contact area (footprint), painting of
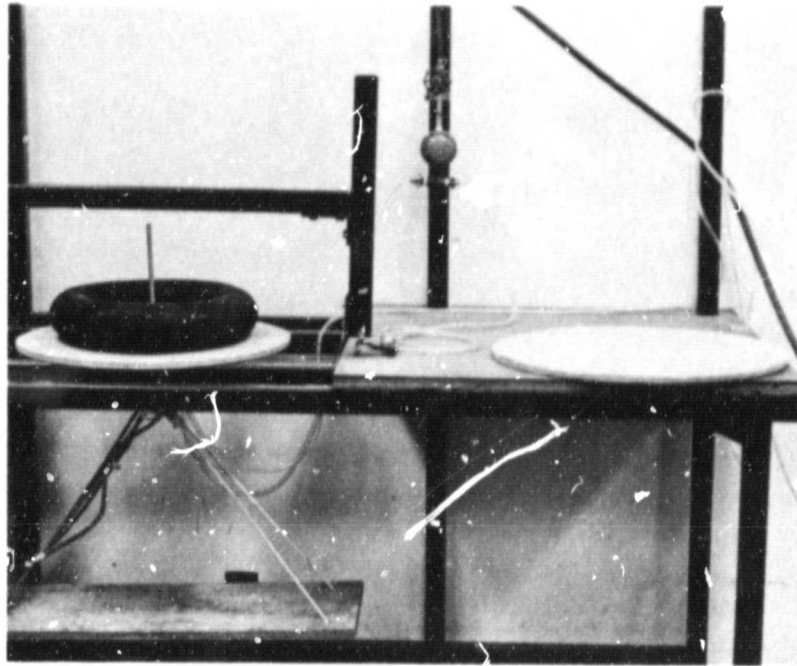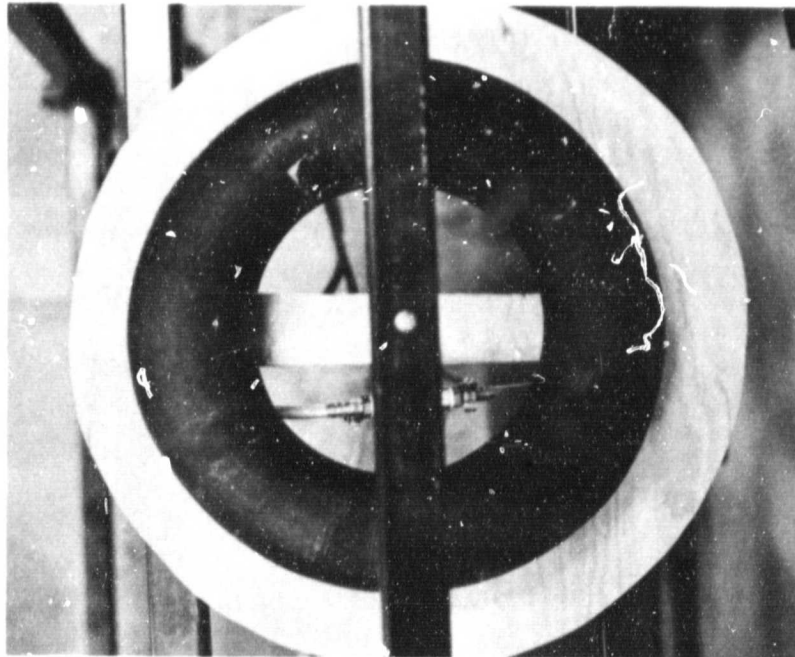
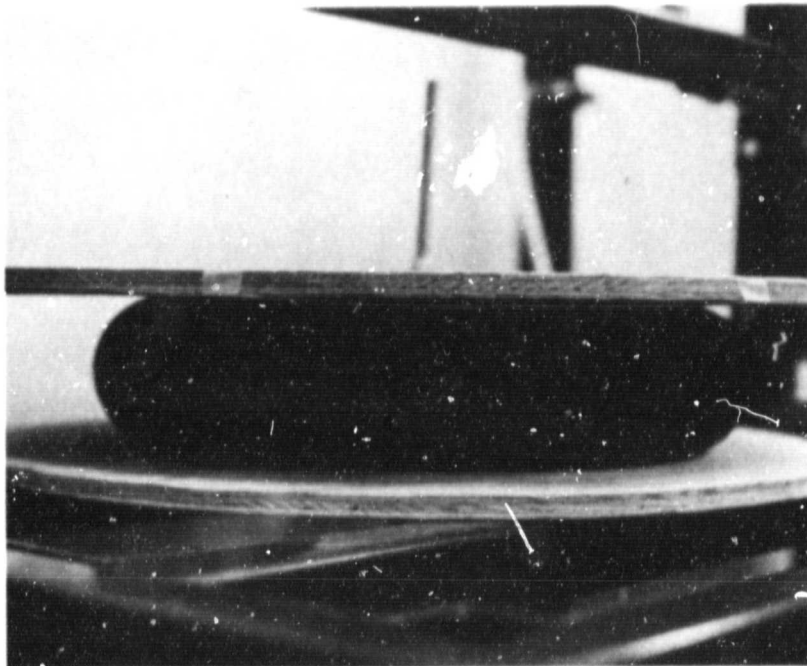Figure 1. Test fixture

Figure 2. Top view
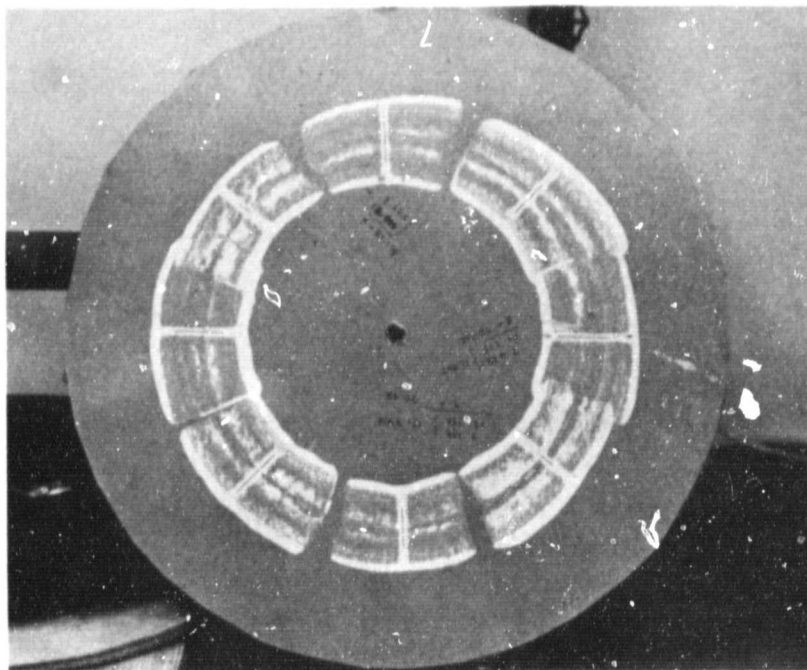
Figure 3.   Loaded horizontal torus

Figure 4.   Footprint area for various loads and
internal pressures

the torus upper surface was completed. Removable craft paper was applied to the underside of the upper load plane. At equilibrium, a painted record of the contact area was left on the craft paper as shown in Figure 4. Thus, analytically predicted contact area versus load could be compared with experimental values.

Oguoma used the Timoshenko general shell equation to develop an expression for contact area A in terms of load L. He assumed that membrane conditions attained in the torus and admitted to a nonlinear stress material behavior. There resulted the expression,

$$
\begin{aligned}
(F_8 F_2^2 - F_6 F_2 F_1) A^4 &+ (2F_2 F_3 F_8 + F_2^2 F_7 - F_6 F_2 F_4 - F_6 F_3 F_1 \\
&- F_5 F_2 F_1) A^3 + (F_9 F_1^2 + 2F_2 F_3 F_7 + F_8 F_3^2 - F_6 F_3 F_4 \\
&- F_5 F_2 F_4 - F_5 F_3 F_1) A^2 + (2F_1 F_4 F_9 + F_3^2 F_7 - F_5 F_3 F_4) A \\
&+ F_4^2 F_9 = 0 \quad \dots
\end{aligned}
\tag{1}
$$

where the F_i terms involved the original torus dimensions, material properties, inflation pressure, and load L. Comparison of analytical results from equation (1) and experimental results is shown in Table I below.

			4.80" x 8" Torus		8.00" x 20" Torus	
Test No.	P_0 (in.)	Load L (lbs)	Area (exp) (sq. in.)	Area (calc.) (sq. in.)	Area (exp) (sq. in.)	Area (calc.) (sq. in.)
1	1.0	25.02	9.13	37.08	25.07	51.81
2	1.0	58.28	36.52	56.55	35.68	81.71
3	1.0	75.02	45.65	63.19	44.42	92.13
4	1.0	108.28	61.96	73.20	83.10	107.86
5	1.0	158.28	70.92	84.41	111.92	125.54
6	1.0	208.28	81.18	93.01	116.89	139.15
7	1.0	258.28	92.34	100.05	139.42	150.34
8	0.5	25.02	19.34	41.83	29.05	59.84
9	0.5	58.28	49.20	58.54	46.38	85.42

Table 1 continued

Test No.	P_o (in.)	Load L (lbs)	4.80" x 8" Torus		8.00" x 20" Torus	
			Area (exp) (sq. In.)	Area (calc.) (sq. in.)	Area (exp) (sq. in.)	Area (calc.) (sq. in.)
10	0.5	75.02	55.08	64.29	77.66	94.23
11	0.5	108.28	67.89	73.02	98.66	107.63
12	0.5	158.28	78.44	82.88	114.21	122.81
13	0.5	208.28	86.74	90.50	130.93	134.60
14	0.5	258.28	91.87	96.75	144.86	144.32

TABLE I

4. DEFLECTION AND CONTACT AREA OF A STANDING TORUS

Gassman [7] initiated the experimental and analytical study of the standing torus under vertical loading. His test fixture is shown in Figures 5 and 6, illustrating the horizontal loading plane below the torus. This loading plane was made from plexiglass so that contact area (footprint) could be measured (Fig. 6). The loading platform, suspension cables, and pulleys are clearly shown in the figures. Referring to Figure 7, the dimensions of the torus are given. The deflection is δ. The vertical height of the center of the torus to the plane in contact may be related as

$$Q = a + b - \delta \tag{2}$$

The final torus volume is derived as a function of the initial torus dimensions and the deflection by

$$
\begin{aligned}
V = {}& \pi(a + b) \left[(.5a + b)(4b^2 + 4ab)^{\frac{1}{2}} - \frac{(4b^2 + 4ab)^{3/2}}{3(a + b)} \right. \\
& + \frac{(.5ab + b^2)}{a + b}(4b^2 + 4ab)^{\frac{1}{2}} \\
& \left. - \frac{(2a^2b + a^3)}{2(a + b)} \, LN \left| 2(4b^2 + 4ab)^{\frac{1}{2}} + 2a + 4b \right| \right] \\
& - \pi(a + b) \left[\frac{Q + b}{2}(Q^2 + 2bQ + b^2 - a^2)^{\frac{1}{2}} \right. \\
& - \frac{(Q^2 + 2bQ + b^2 - a^2)^{3/2}}{3(a + b)} + \frac{(bQ + b^2)}{2(a + b)}(Q^2 + 2bQ + b^2 - a^2)^{\frac{1}{2}} \\
& \left. - \frac{(2a^2b + a^3)}{2(a + b)} \, LN \left| 2(Q^2 + 2bQ + b^2 - a^2)^{\frac{1}{2}} + 2Q + 2b \right| \right]
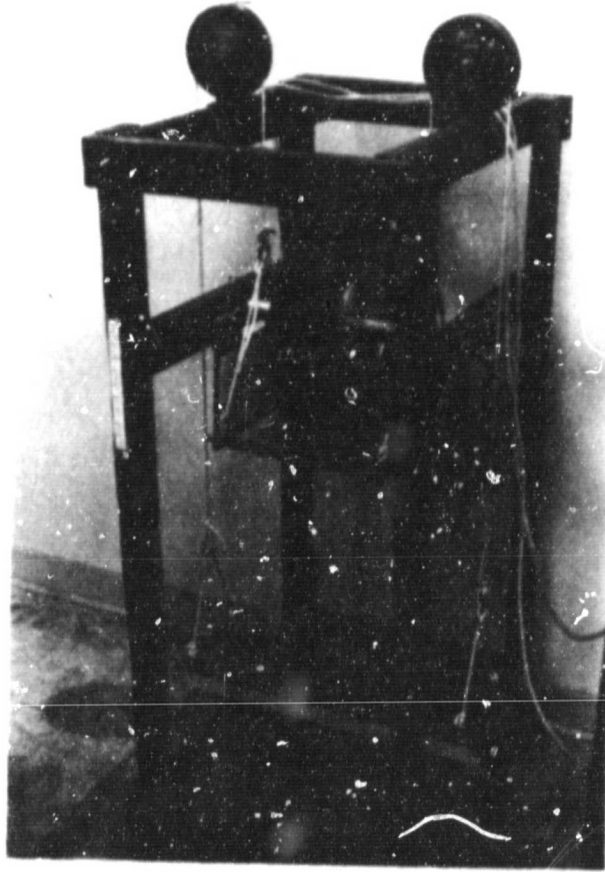\end{aligned}
\tag{3}
$$

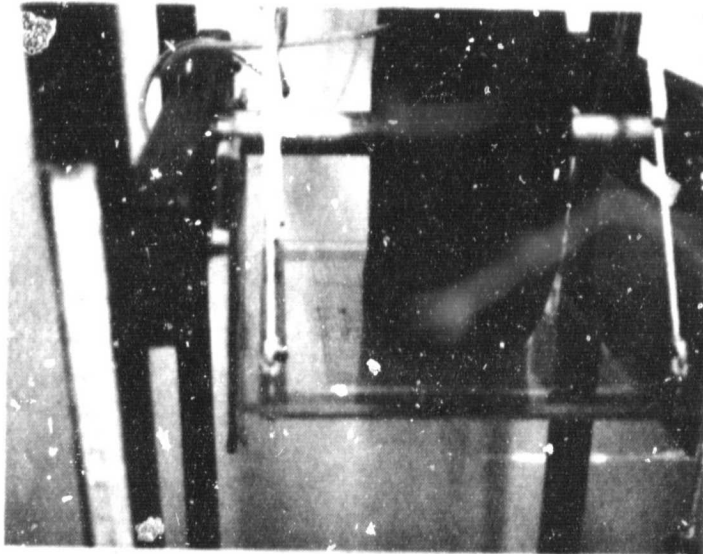Figure 5.   Torus mounted on test frame.
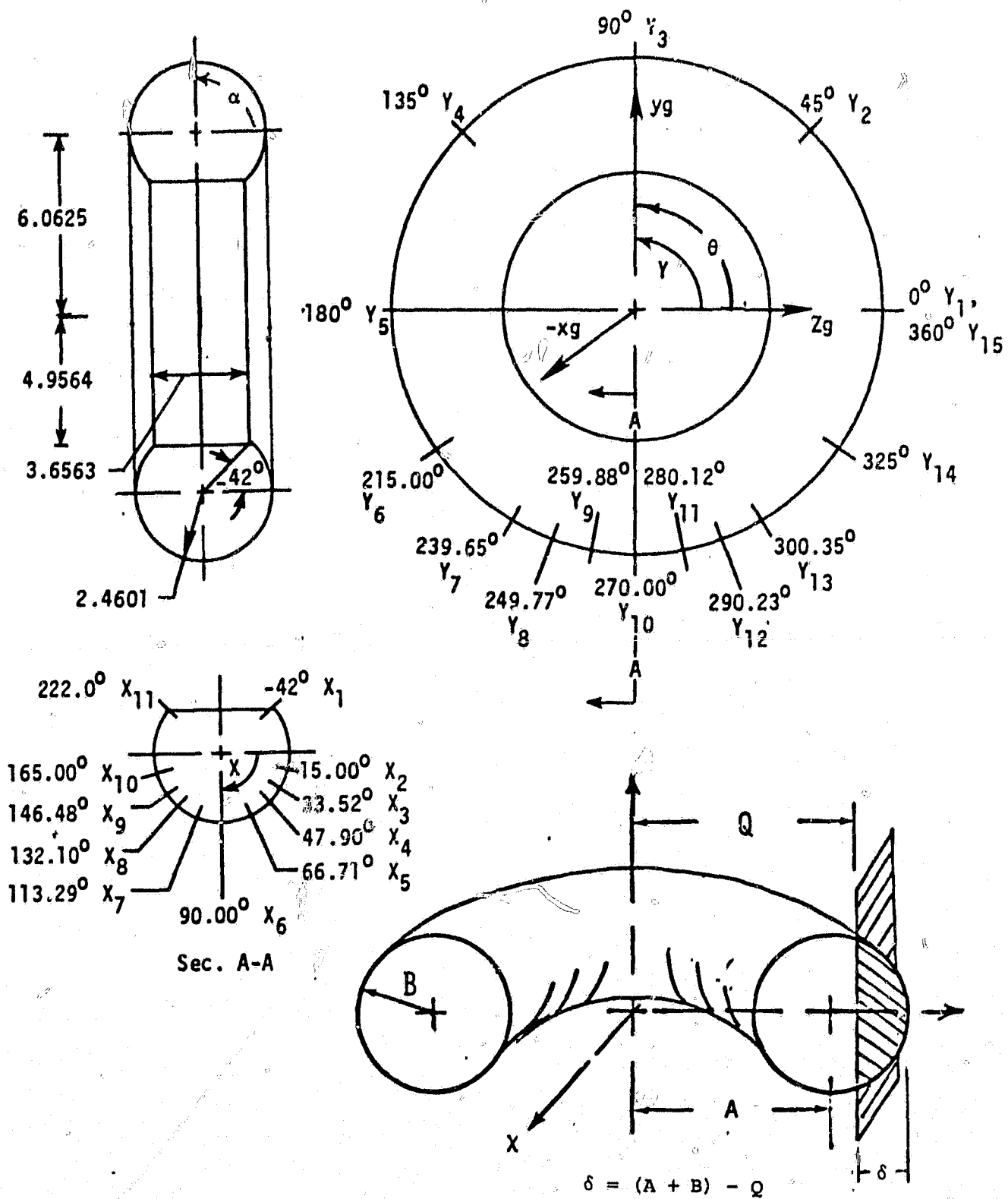

Figure 6.   Loaded torus exhibiting bulge.

Figure 7.   Torus dimensions and global coordinate set.

Finally, the torus volume, load, and initial dimensions and pressures are related to the deflection as shown below.

$$\left(1 - \frac{V = V(a,b,\delta)}{2\pi^2 b^2 a}\right)\left(\frac{L}{\pi\delta[(2b - \delta)(2a + 2b - \delta)]^{\frac{1}{2}}}\right) = (P_i + P_a) \quad (4)$$

The contact area as a function of deflection and torus dimensions can be derived as

$$A = \pi\delta\left[(2b - \delta)(2a + 2b - \delta)\right]^{\frac{1}{2}} \quad (5)$$

The load deflection relationship given in Equation 4 can be solved by iterative numerical techniques and the footprint area can be found as a function of deflection δ from Equation 5. A computer program was written and analytical solutions were found for torus deflection from the load L by use of Equation 4. These values were compared to experimental results and will be discussed in the following section.

5. FINITE ELEMENT ANALYSIS OF A STANDING TORUS

Mack's contribution to the project consisted of application of the finite element analysis to the standing torus. STAGSC computer code was exploited in the analytical prediction of deflection and strain versus vertical load of the torus. Some of the difficulties of the classical formulation of this problem can be overcome in a finite element approach. This approach is advantageous when the geometry of the structure is irregular and the boundary or loading conditions are arbitrary. Consequently, the bulging in the sidewalls and the unsymmetric loading conditions present no difficulty here.

Considerable work was involved in the correct exploitation of modeling strategies. A comparison was made of final results of deflection and strain (1) between a linear material model and a nonlinear material model; (2) between linear and nonlinear structural geometries allowed from incremental loading; and (3) between coarse and fine grid configurations describing the meridional and circumferential coordinates.

One of the most important modeling considerations was the exploitation of symmetry. Figure 8 shows a quarter torus under a load of 114 N. The STAGS model used in this computation displayed a 13 x 15 grid configuration distributed over one-fourth of the structure. Comparison showed that the node density from this model was four times greater than that given by a 13 x 15 grid devoted to the entire structure, while the number of degrees of freedom is the same. Note in Figure 8 that the contact area approaches a flat plane and the sidewall near the base of the tire exhibits a bulge. Close inspection of the figure shows that the deformed grid array is superimposed on the underformed grid, plotted
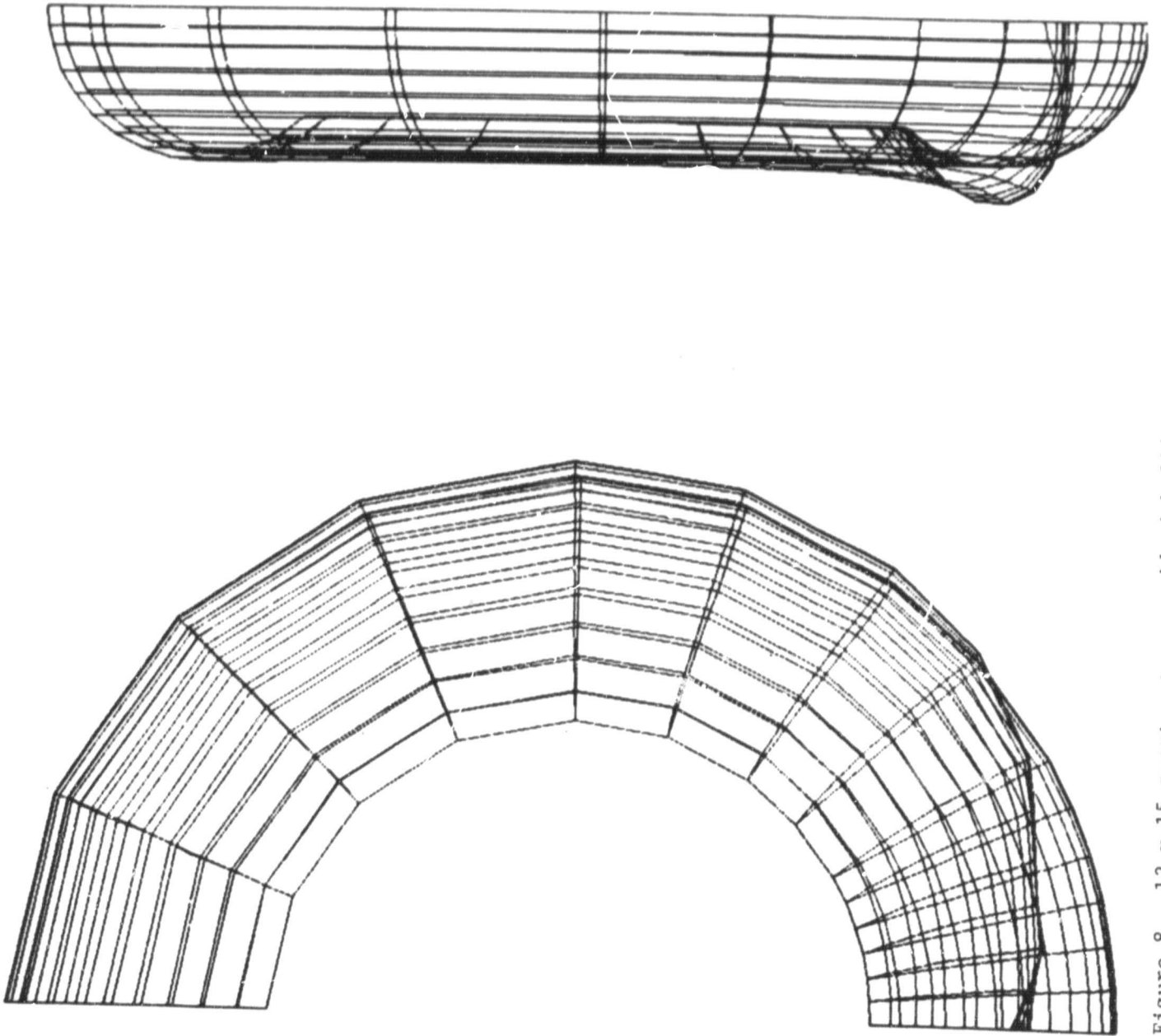
Figure 8. 13 x 15 quarter torus grid with 114 N load.

before vertical loading of the plane into the torus.

The STAGS numerical procedure produces computed values of circumferential stress σ_θ and meridional stress σ_ϕ, as well as strains in these two directions, within each grid point defined by the user. Figure 9 is a plot of the circumferential stress distribution over the quarter torus grid configuration. These computed values show a high degree of stress reversal, from tensile stress in the region of the sidewall bulge to a high level of compressive stress in the footprint region, with a sudden reversal to tensile again. Strain computations indicate the same displacement reversal, and close examination of Figure 8 indicates a buckling or snap-thru behavior of the structure wall. This condition is verified in the photograph of Figure 10, the actual footprint of a heavily loaded torus. The negative curvature near the center of the footprint might well resemble the condition in a tire under a large vertical load. Negative curvature in the center of the footprint has some important implications. Generally, the footprint area increases under increasing load. The braking force of an aircraft tire is directly dependent on footprint area. Local snap-thru in the contact area actually decreases the contact area at high vertical load conditions.

Figure 11 compares the computed torus deflection versus vertical load and the experimentally observed deflection. The solid curve of Figure 11 was plotted from Gassman's analysis, given earlier as Equation 4. The deflections computed from finite element analysis are seen to compare well with the analytical results of Gassman. As the grid density of the finite element procedure increases, the computed deflection approaches the experimentally observed deflection. Several conclusions
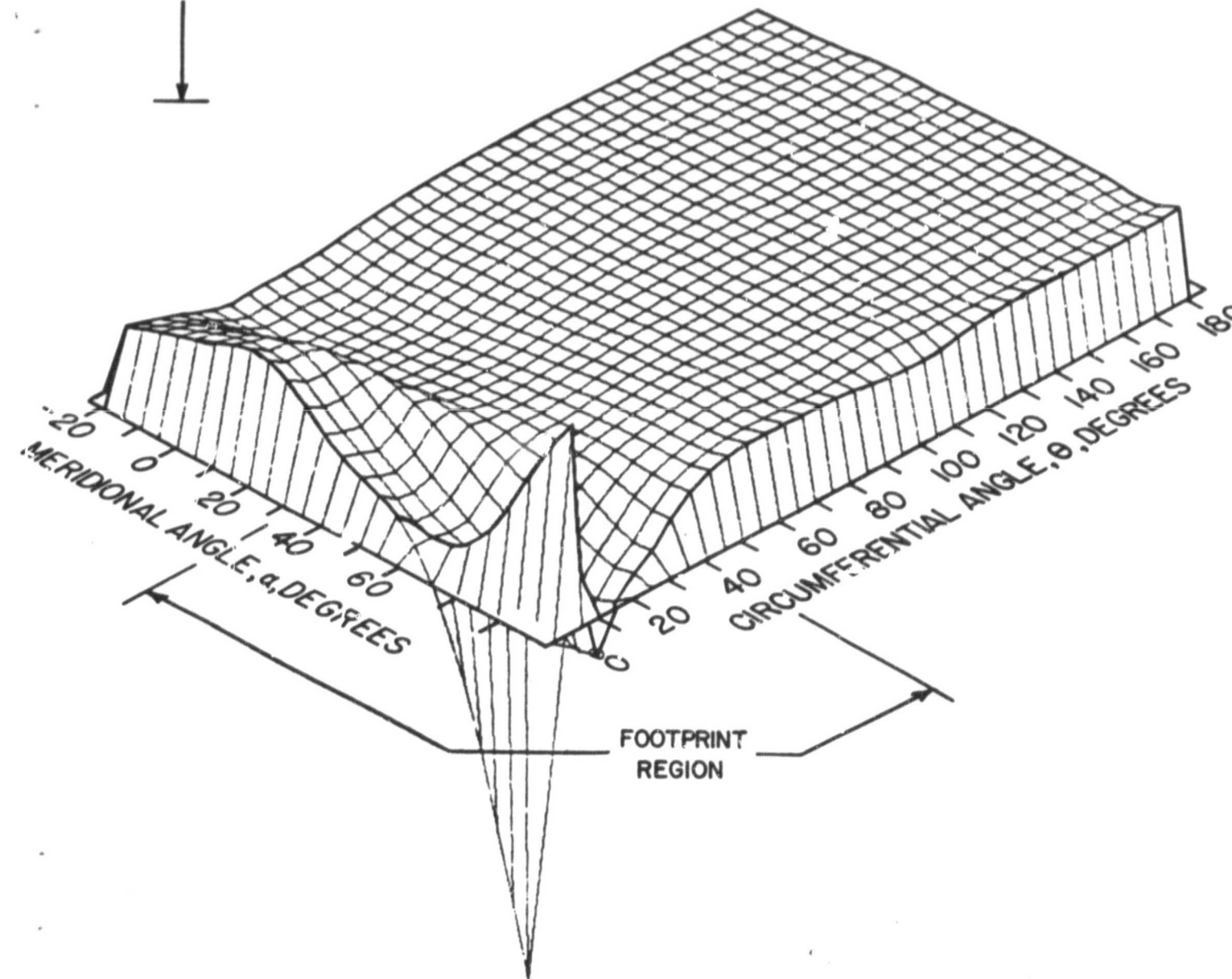
345×10^3 Pa

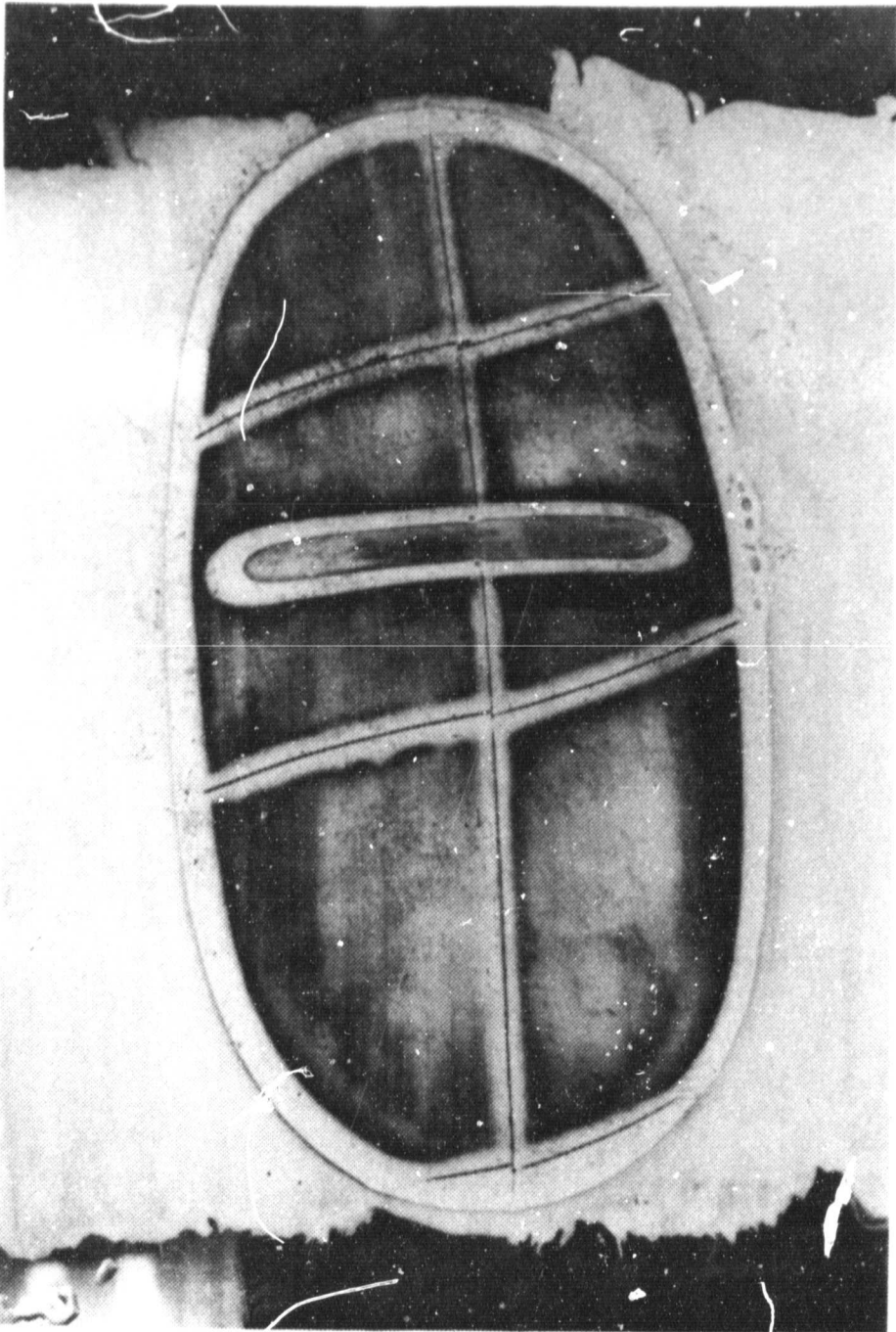Figure 9. Circumferential stress distribution, σ_θ, at 114 N load.

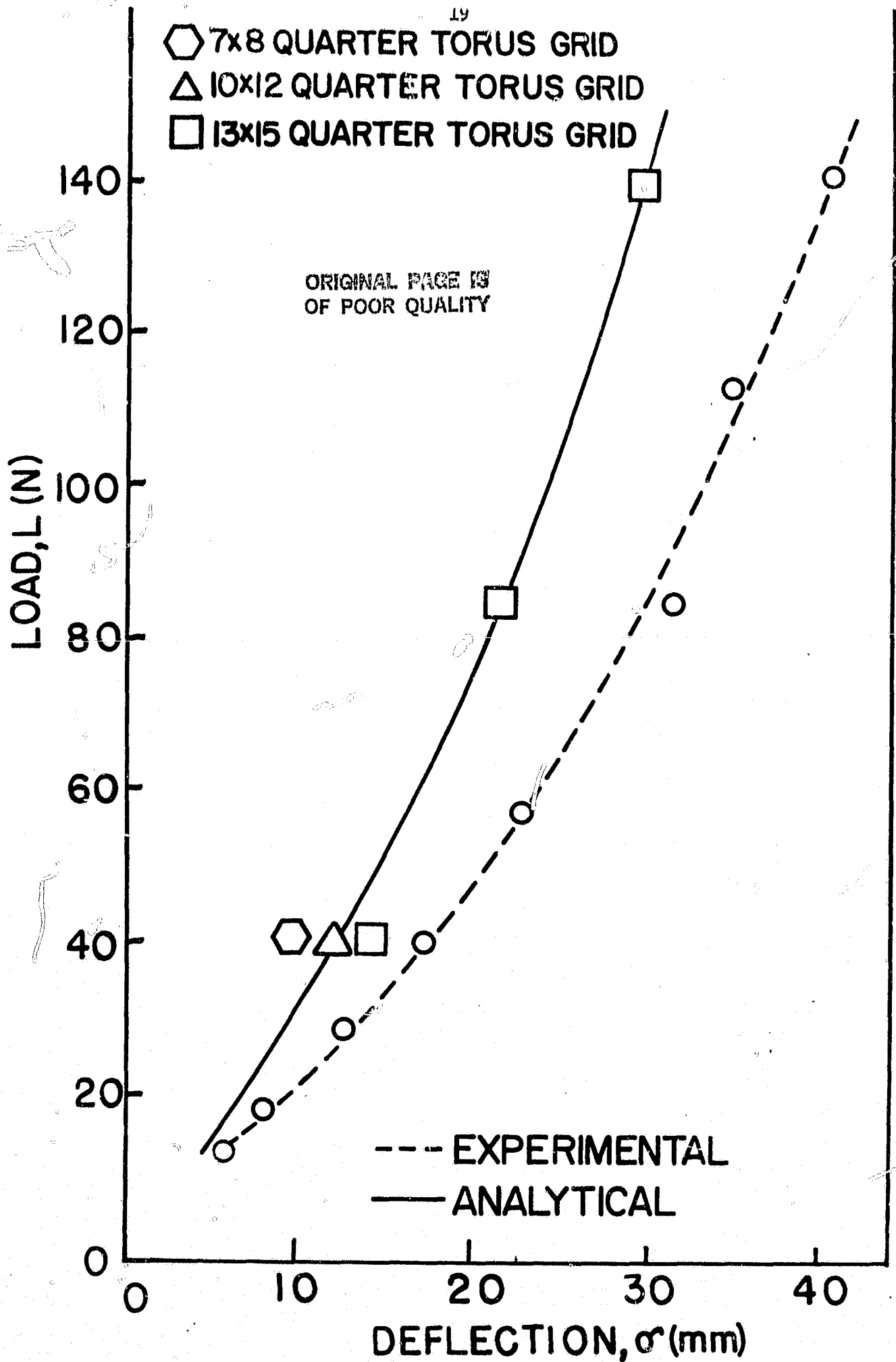Figure 10.   Footprint of an inner tube showing negative curvature.

Figure 11. Load-deflection curves for analytical, finite element, and experimental data for torus at $P_i = 3.45$ kPa.

are apparent; a finite number of coordinates always overestimates the

stiffness of the structure and one must compromise between computational

cost and desired accuracy of the finite element results.

6. EXPERIMENTAL STRESS ANALYSIS OF A
THIN-WALLED TORUS UNDER VERTICAL LOAD

Hill applied mercury filled rubber strain gages to the wall of the standing torus and measured the resulting strain in the structural wall at various coordinates and under various load conditions. Figure 12 is a photograph of the liquid metal filled strain gage and Figure 13 is a photograph of the strain gage calibration device together with ballast circuitry and amplifiers. Figure 14 shows some typical gage placement at zero degrees meridional coordinate. Hill had altered the test fixture to allow easy variability of the circumferential angular setting of the torus. The automated data collection system shown in Figure 15 allowed computer acquisition, analysis, and storage of strain readings at the many coordinate nodes used in the computational torus grid. Figure 16 shows a plot of the experimentally measured strains and compares these values with the computed results of Mack at the same meridional angle and load conditions. It is seen that computed and measured strains ϵ_θ agree well at this meridional angle but that measured meridional strains depart markedly from computed values. This coordinate places the strain gage at its closest proximity to the tire rim. Good agreement was achieved between measured and predicted meridional strain in the area of the torus away from the rim. The boundary condition at the rim allowed no rotation or translation; the torus was held clamped at the rim in the computations presented here. It was concluded that this assumption of clamped boundary must be modified to better model the actual conditions of the torus on the steel rim.
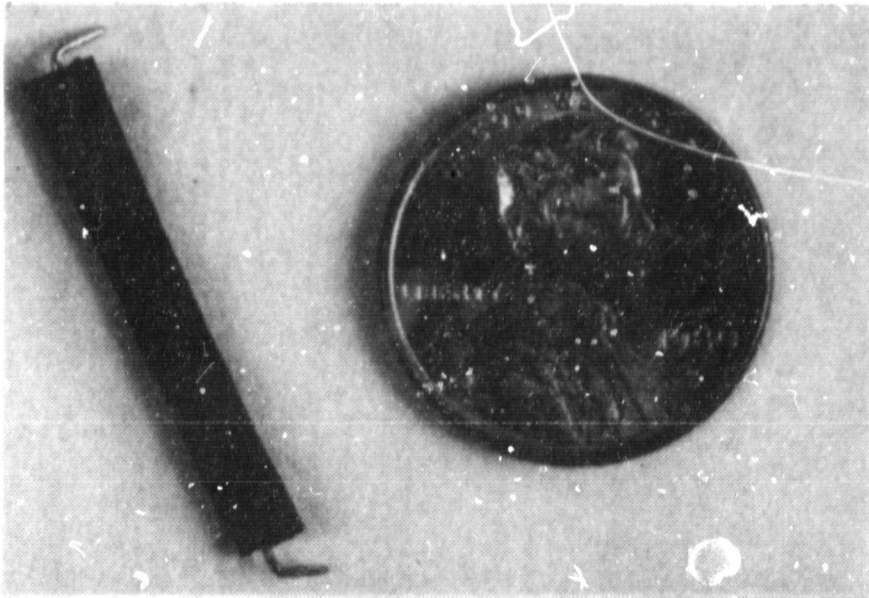
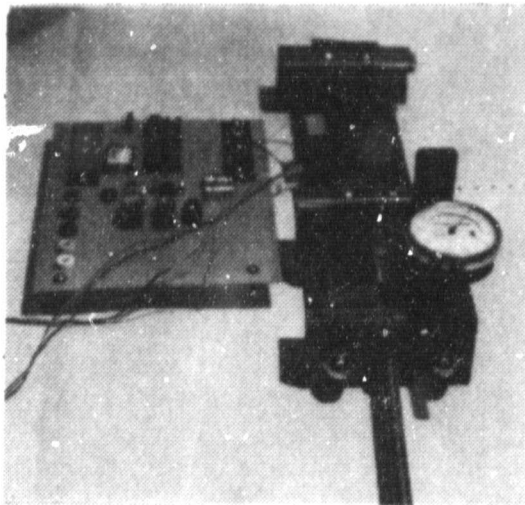Figure 12. Firestone liquid metal gage

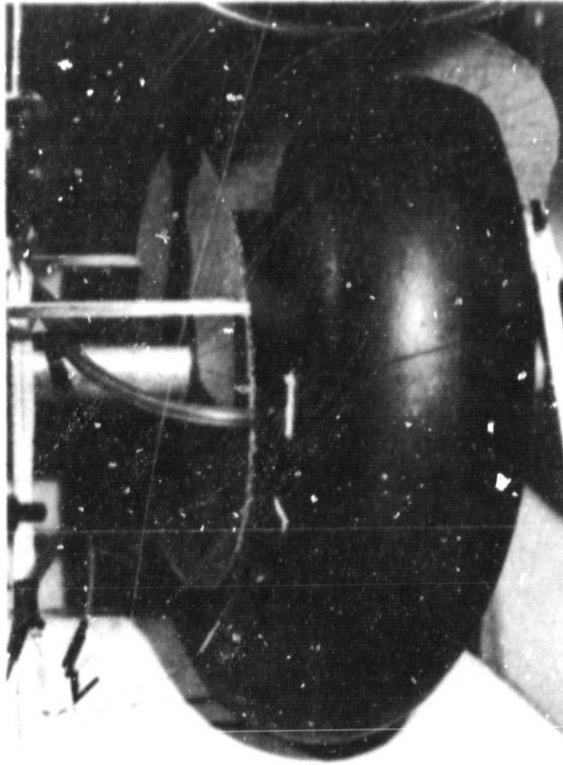Figure 13. Calibration device

Figure 14.   Gage placement at zero
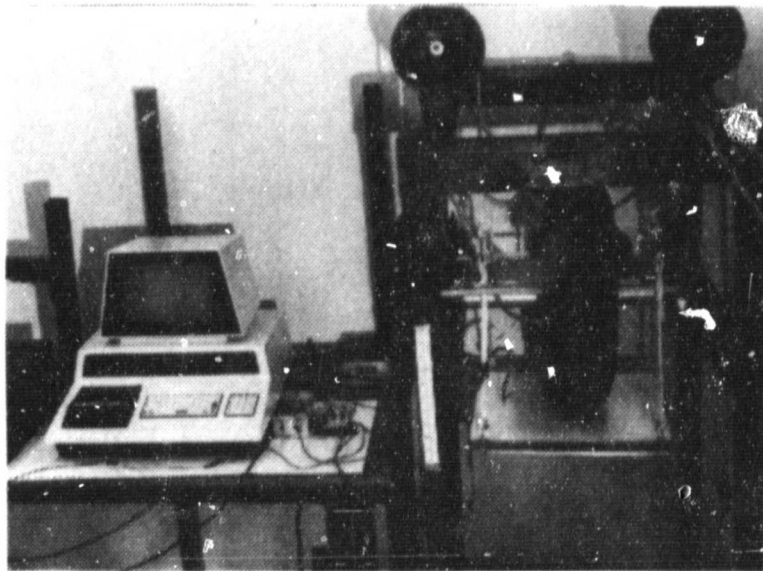degrees meridional angle

Figure 15.   Complete system with
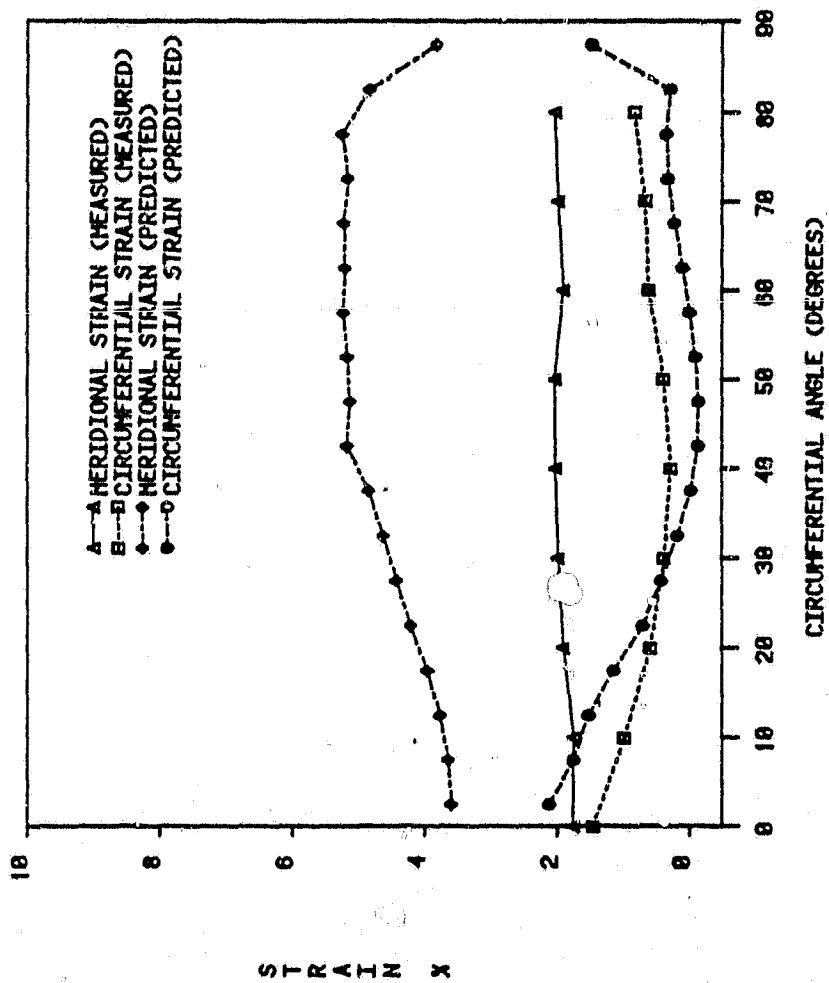data acquisition

ORIGINAL PAGE IS
OF POOR QUALITY

Figure 16. Comparison of measured and computed strains using a fixed rim boundary. P_i = 3.45 kPa, load L = 35 N.

7. A STUDY IN RIM BOUNDARY MODELING

Bucher has modified the model of the torus at the rim. As stated above, the original modeling strategy fixed all 6 degrees of freedom, 3 translations and 3 rotations, at the rim boundary. The result of this boundary definition is given in Figure 16. This series of data are at a meridional value of -10.0° to correspond with Hill's results. Examination of these data show that a clamped rim boundary predicts strains circumferentially well in both trend and magnitude. However, meridional strains are not only overpredicted in magnitude, but have poor trendwise correlation as well. This would indicate that the rim boundary is overconstrained and should be refined. Examination of the literature shows similar overprediction in meridional strain values for other FEM models in which the rim boundary is completely constrained.

Redefinition of the translational boundary conditions was undertaken using a subroutine UCONST. This subroutine allows for linear constraint definitions between degrees of freedom along the boundary. These relationships must take the form:

$$\Sigma C_i X_i = 0$$

where X_i is one of the degrees of freedom and C_i is constant. Both global horizontal and vertical motion at the rim were examined. Based on the shape of the rim on which the inner tube set, the relationship in Figure 17 was derived for the rim boundary. Initially the value of "alpha" was 42.0° and "beta" was set to 0. As the incremental solution was carried to completion, the rotational value RV was examined and the relationship was updated.
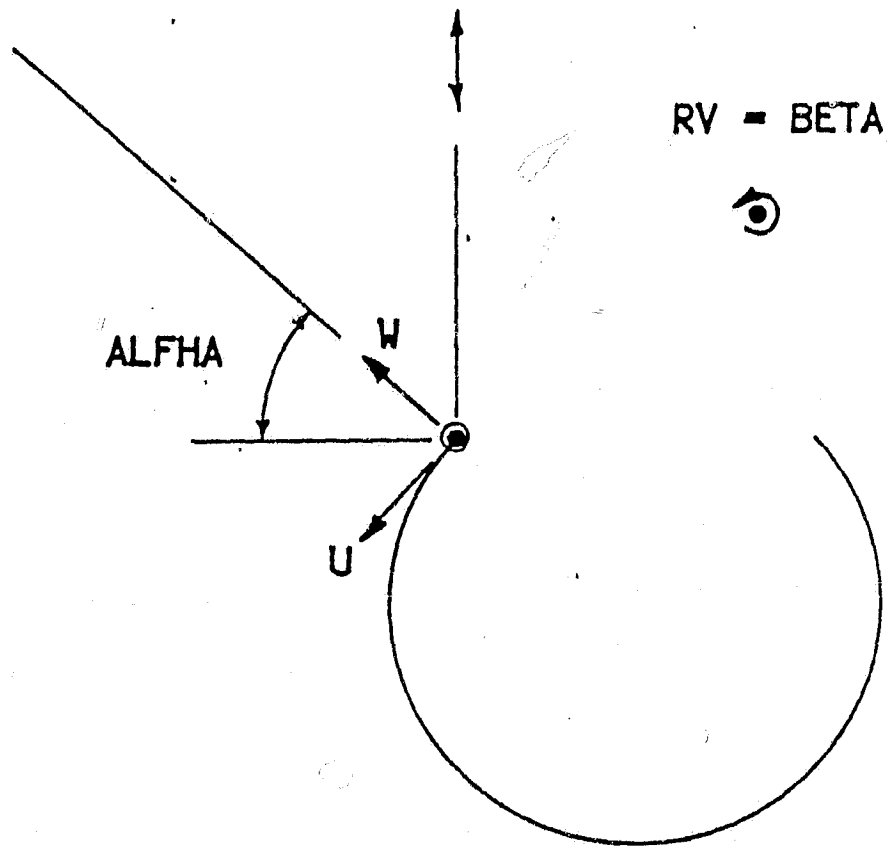
$$W \cos(ALFHA - BETA) + U \sin(ALFHA - BETA) = 0$$

Figure 17. Rim boundary configuration

The results for this strategy are given in Figure 18. While the magnitude of both the meridional and circumferential strains are over-predicted, magnitudes of these overpredictions are about the same in both cases. In addition, both strain predictions now show good trendwise correlation with experimental values. A displacement plot for this strategy is given in Figure 19. Close examination of Figure 19 indicates that, indeed, deflection at the rim has occurred as well as some rotation. The sidewall bulge and footprint deflection are again evident.

Results of the study indicate that modeling the rim boundary as clamped does not give adequate accuracy in strain predictions in the upper sidewall. Use of free rotations and simple linear relationships between the translations leads to more accurate strain predictions in both magnitude and trend than simpler models. The study would reinforce the need for more sophisticated boundary definitions at the rim.
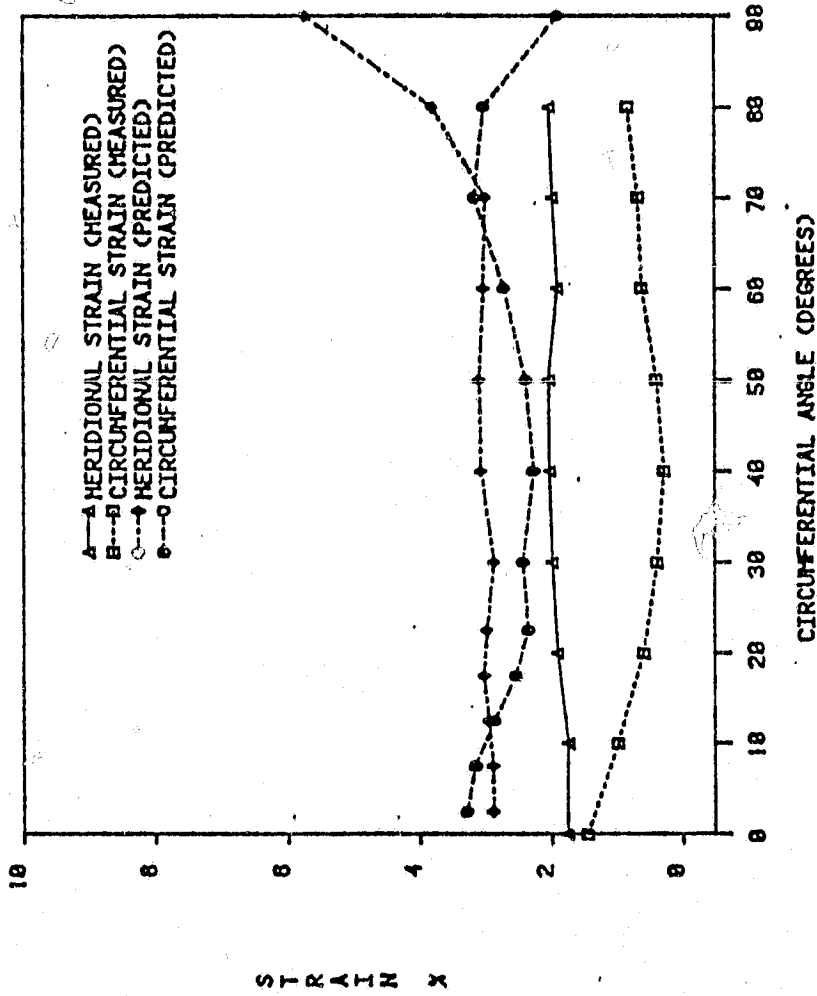
Figure 18. Comparison of measured and computed strains using
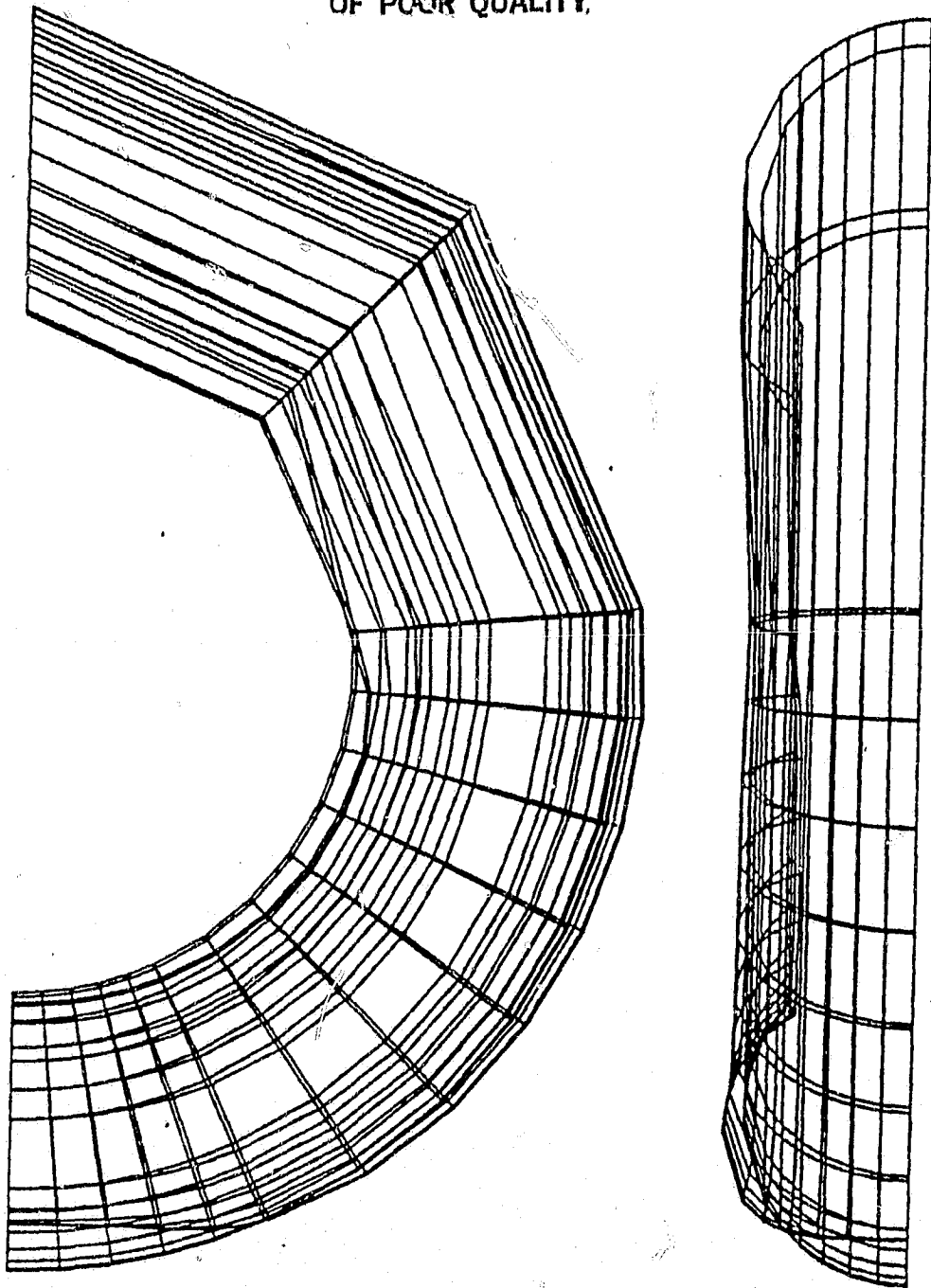a free rim boundary. $P_i = 3.45$ kPa, load L = 35 N.

Figure 19.   Quarter torus with free rim boundary, load L = 35 N.

8. EXPERIMENTAL AND FINITE ELEMENT ANALYSIS OF AN INFLATED TORUS WITH NORMAL AND TANGENTIAL LOADING

Miller altered the test rig shown in Figure 5 so that vertical and braking (tangential) loads could be applied to the torus simultaneously. Figure 20 shows the scheme for adding tangential loading to the existing fixture. Figures 21 and 22 compare the analytical and experimentally resulting vertical and horizontal displacement from the combined load cases. The analysis was accomplished by use of the STAGSCI FEM (finite element method) and compares results at a 70 N (15.7 lb) vertical load. The horizontal load (tangential force) is plotted as a decimal fraction of the 70 N normal load. It is seen from Fig. 21 that vertical deflection did not change as tangential force was increased. The horizontal displacement, however, increased markedly as tangential force increased as seen from Fig. 22. As before, it is seen that the 10 x 21 half torus grid utilized in these calculations has overestimated the structural stiffness and calculated deflections are less than the measured values.

Flugrad and Miller devised a scheme for iteration of the force distribution in the footprint area. In previous analysis completed by Mack, it was necessary to know the final contact area from experimental observation; then the forces in the footprint area were distributed over this region. Figure 23 illustrates the scheme. Several springs of different lengths and different spring rates are suspended from a horizontal beam as shown. The total force exerted upward on the assembly is known and the individual force to be applied to each spring is to be determined so that all springs deflect to a common vertical equilibrium position Z_E. An arbitrary distribution of forces is chosen to begin the procedure. The deflection of each spring is noted and corresponding
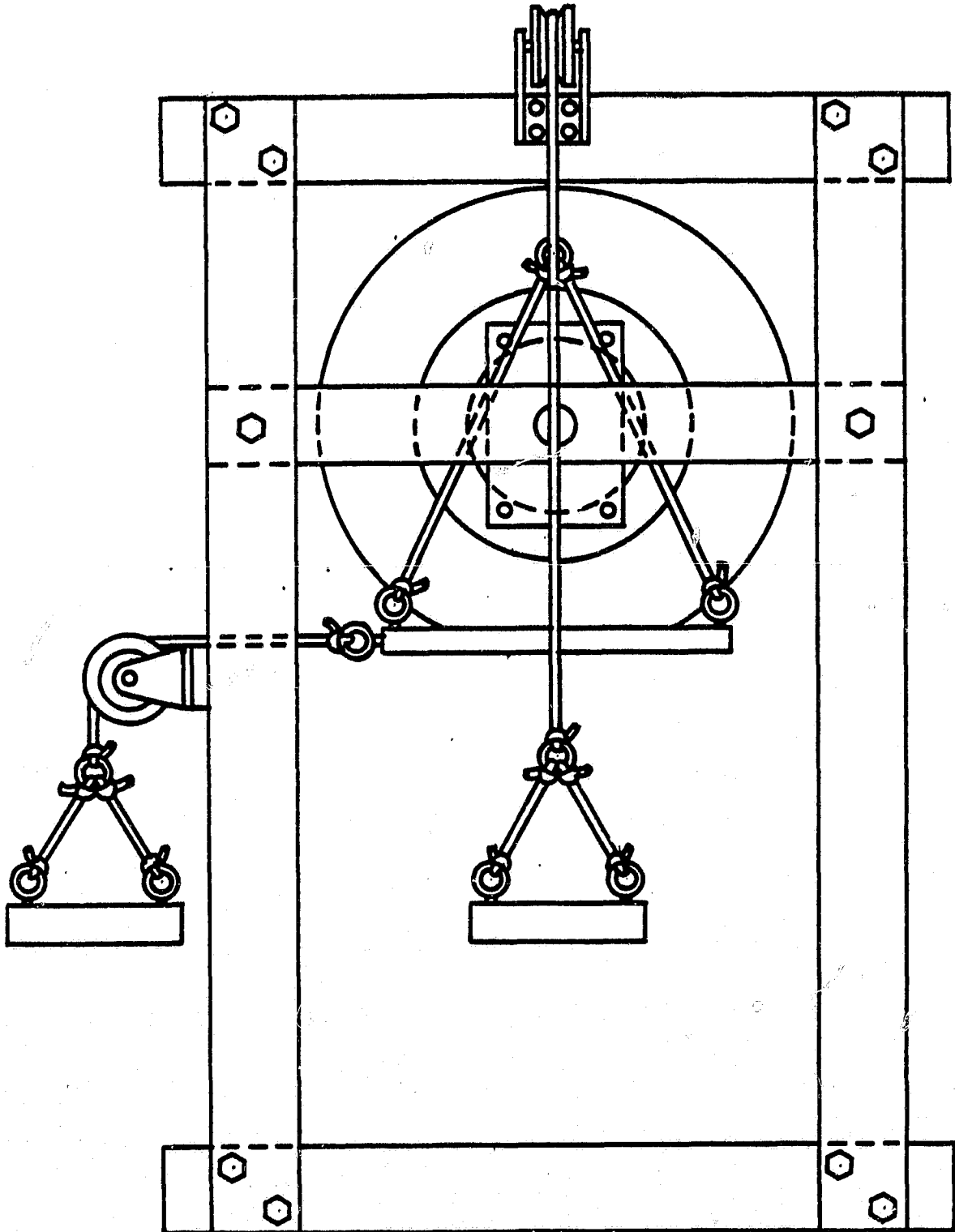
ORIGINAL PAGE IS
OF POOR QUALITY

Figure 20. Test stand modified to apply normal and tangential loads.
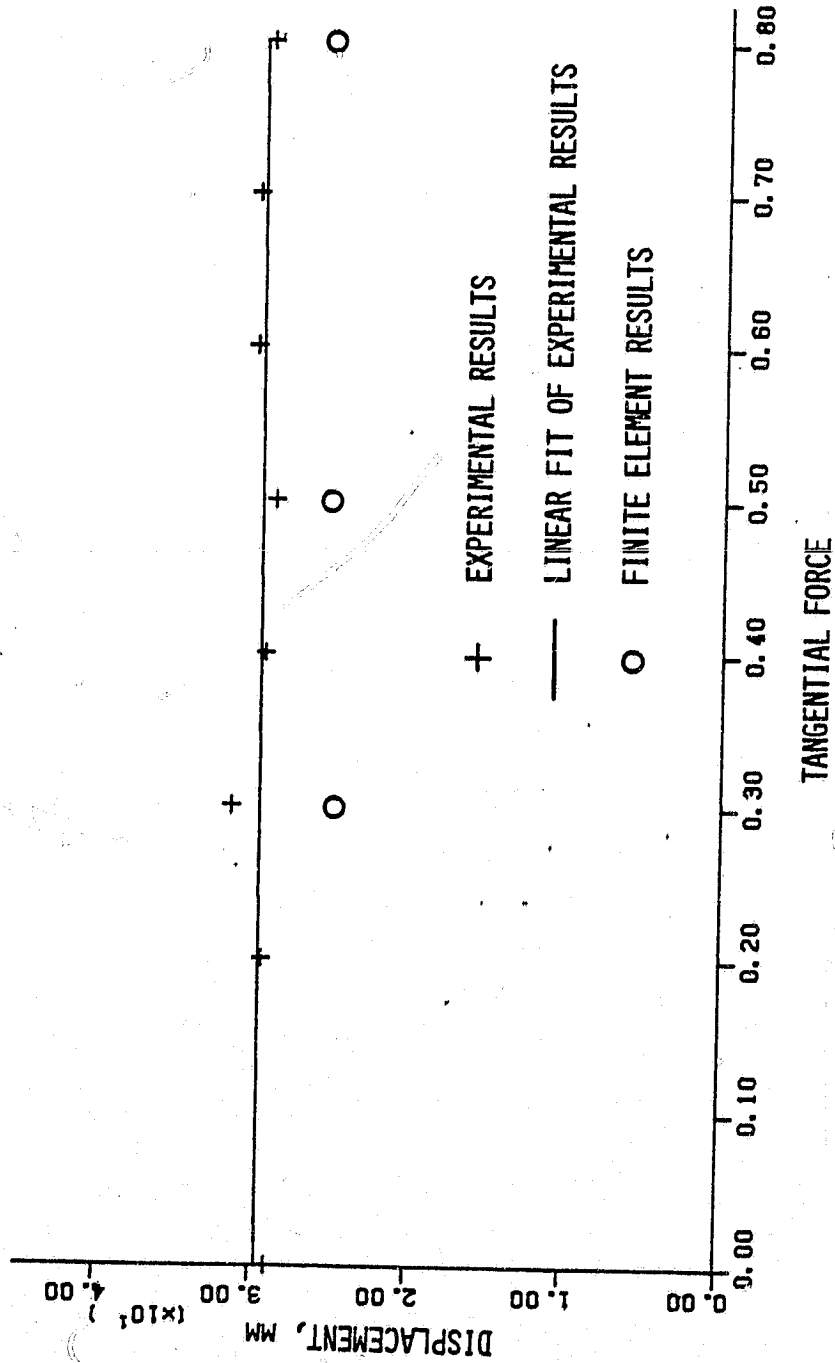
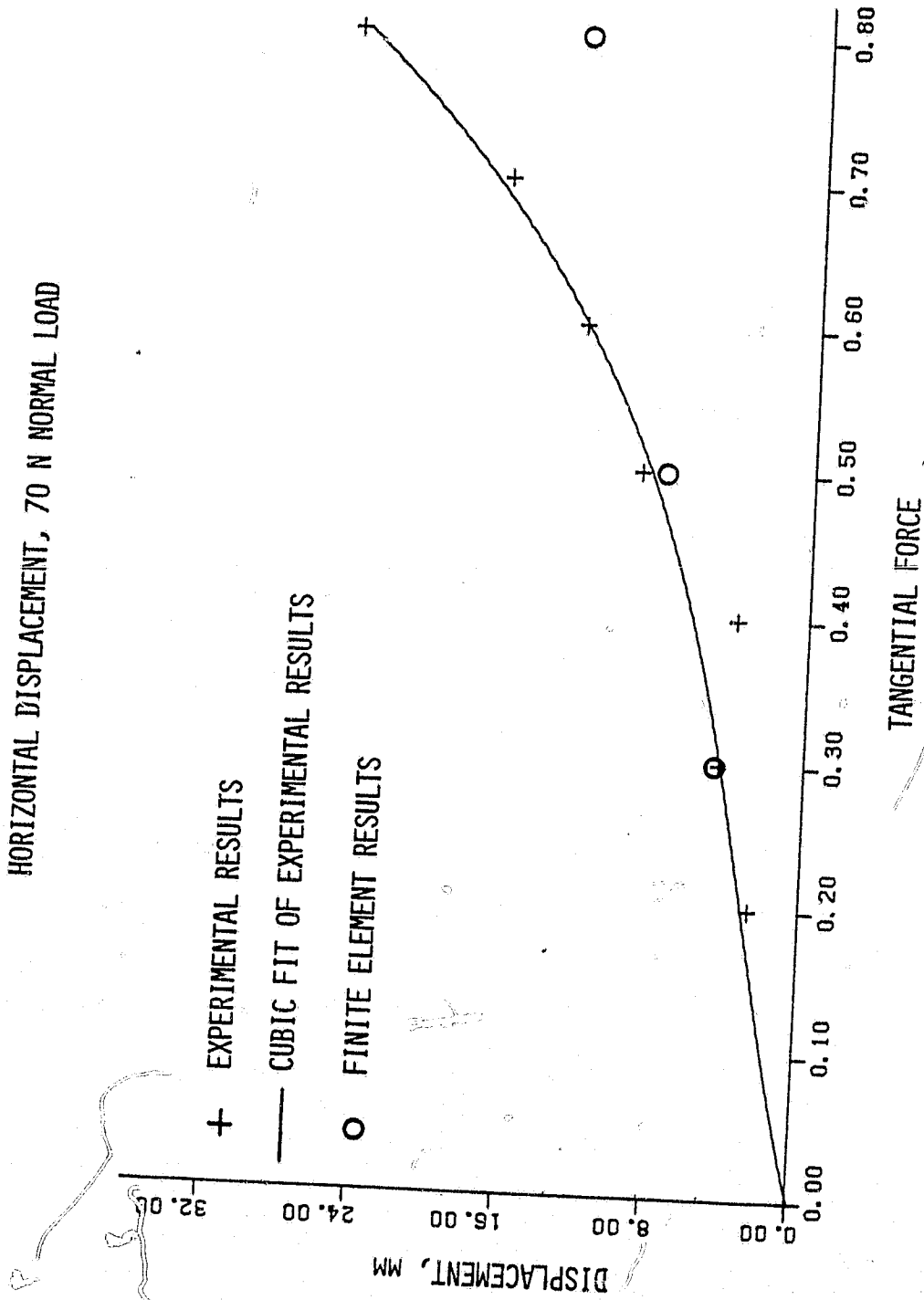Figure 21. Vertical torus displacement as a function of tangential force, normal load
L = 70 N.

Figure 22. Horizontal torus displacement as a function of tangential force. Normal load L = 70 N.
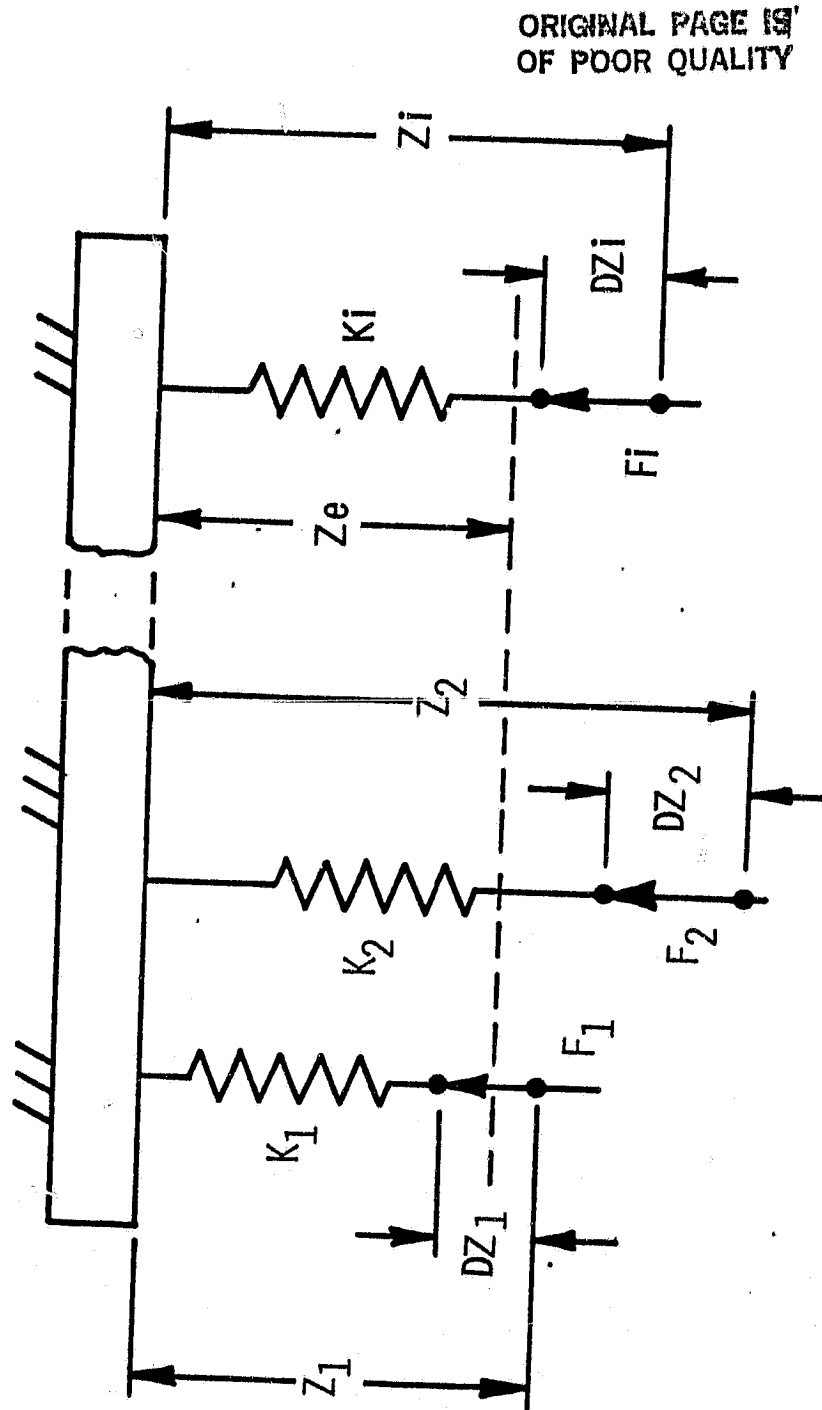
Figure 23. Iterative scheme for contact force redistribution to find equilibrium position Z_E

spring rates are calculated. Since total force is known, the equivalent
common equilibrium position Z_E is calculated from the formula given in
the figure. The procedure then calculates the individual force F_i from
known K_i and Z_E and these forces are distributed over the footprint in
the next FEM iteration. Figure 24 is an FEM plot of the iterated results
after three trials. It is seen that a flat footprint results and that
considerable horizontal deflection is evident from the braking force.

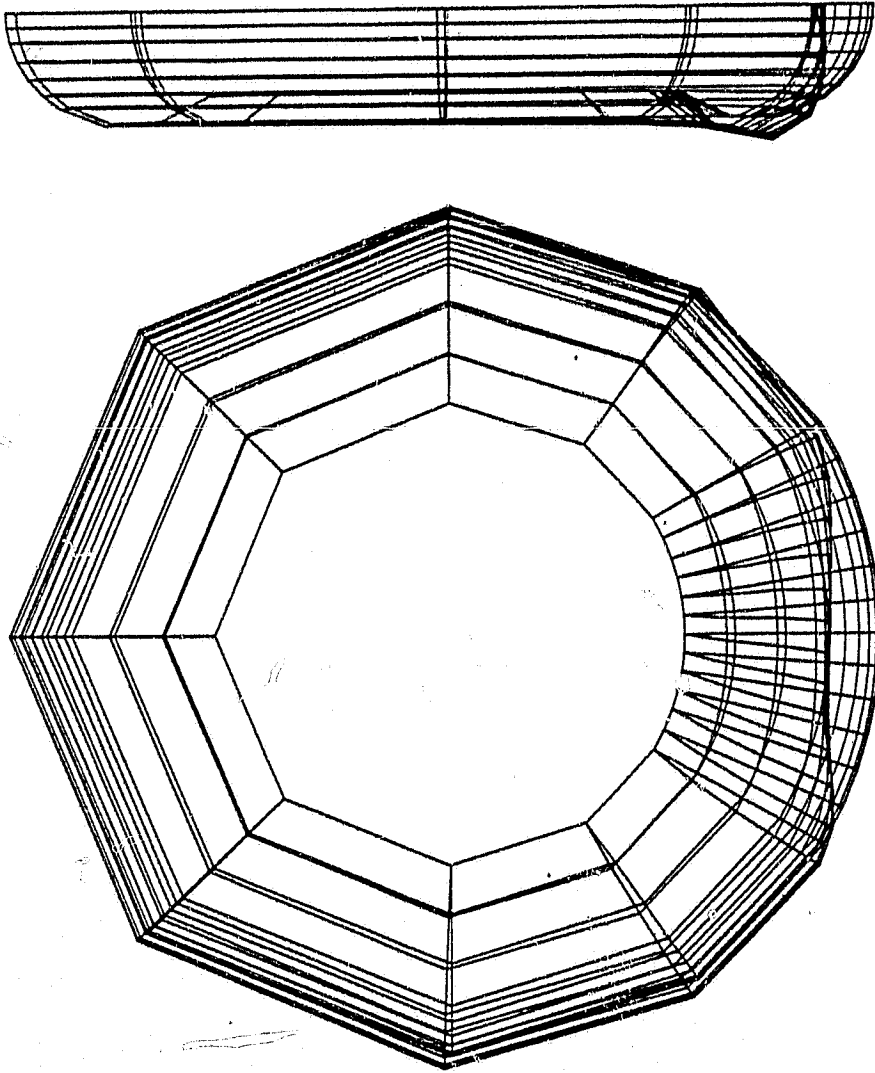SIX NODE CASE, HALF TORUS, 70 N NORMAL, 80% TANGENTIAL, FINAL RUN

Figure 24. Final equilibrium position of torus with combined normal and tangential load.

9. AN EXPERIMENTAL AND FINITE ELEMENT ANALYSIS OF AN INFLATED TORUS WITH NORMAL AND LATERAL LOADING

Under the advice and guidance of D. R. Flugrad, Pau has adapted the test rig to allow combined normal and lateral (cornering) loads to be applied to the inflated torus. The clear plexiglass loading platform has been removed from below the inner tube and mounted on top as seen in Figure 25. A close-up view is shown of the parallel four-bar linkage used to constrain the transparent plastic plate to remain horizontal over the torus. The slots in the lower links allow the plate to slide freely in a horizontal direction. A turnbuckle on the test stand allows the ganged four-bar linkage to hook the plate in the up position in order to set the plate's vertical datum plane. Thus the normal load is now applied downward from above the torus. This was done to facilitate photographing the contact area and to eliminate the need for pulleys to reverse the load direction from applied weights.

Test results indicate that vertical deflection increased as the lateral load was increased. The plot of this vertical sinking distance versus the lateral load is given in Figure 26. The lateral deflection of the torus as a function of the lateral load is plotted in Figure 27. The torus' lateral deflection appears to be independent of the normal load applied. Photographs of the contact area are shown in Figure 28. Considerable eccentricity of the combined loaded torus is apparent with significant shift in the footprint center. Considerable buckling in the torus sidewall at higher normal and lateral loads was observed during testing.

Finite element analysis of this combined loading condition was completed using STAGSC1. The problem was found to be sensitive to the
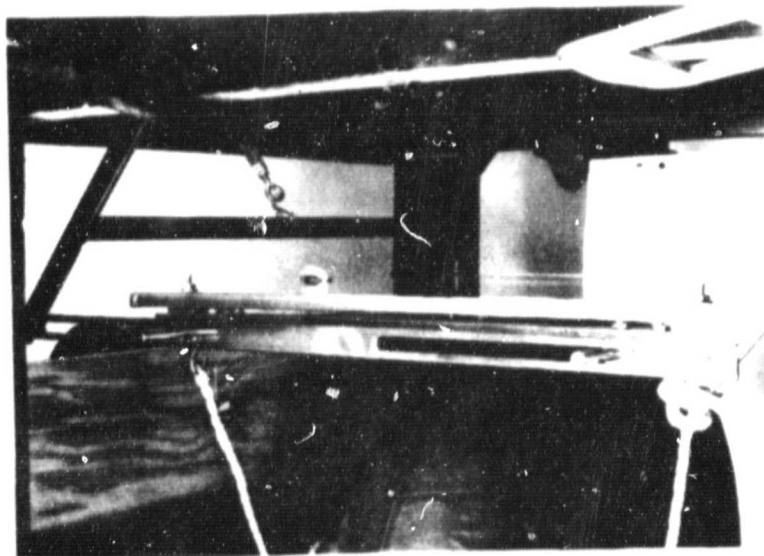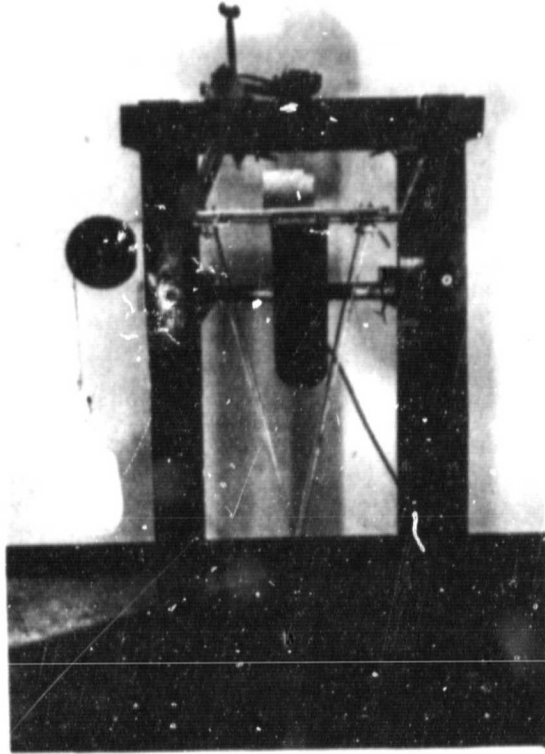
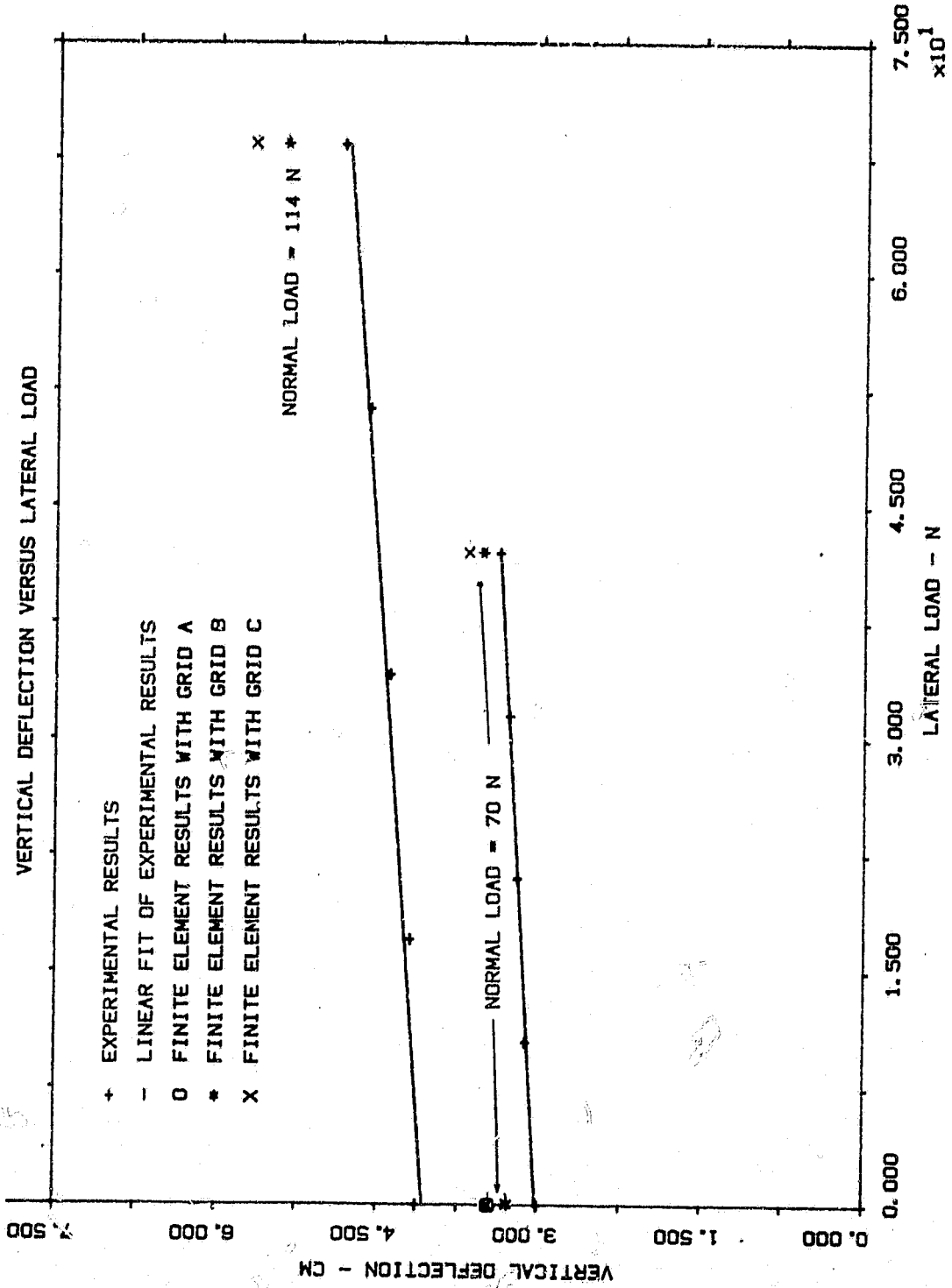Figure 25.   Experimental test fixture with plate linkage system.

FIGURE 26.   Vertical Deflection versus Lateral Load
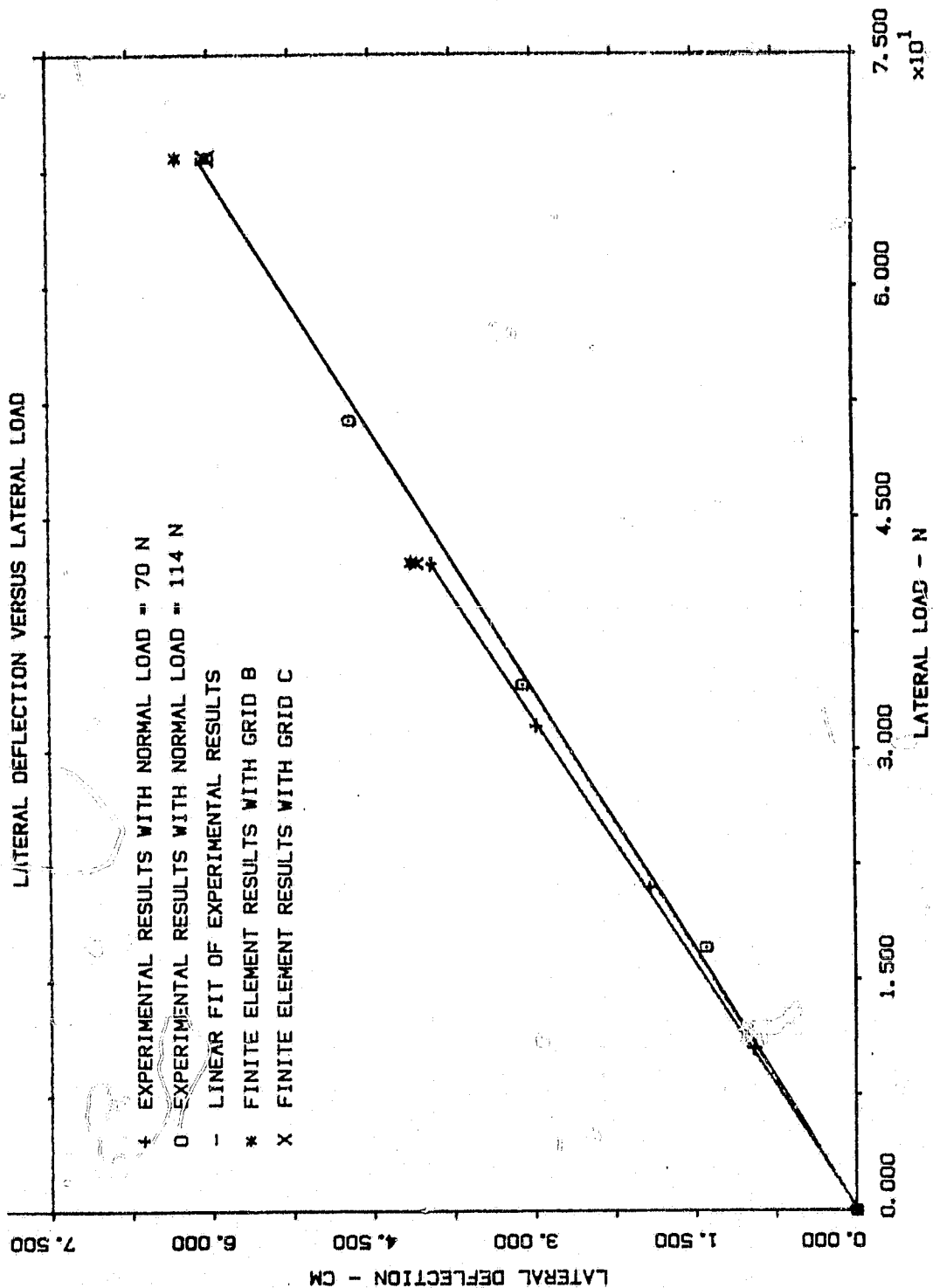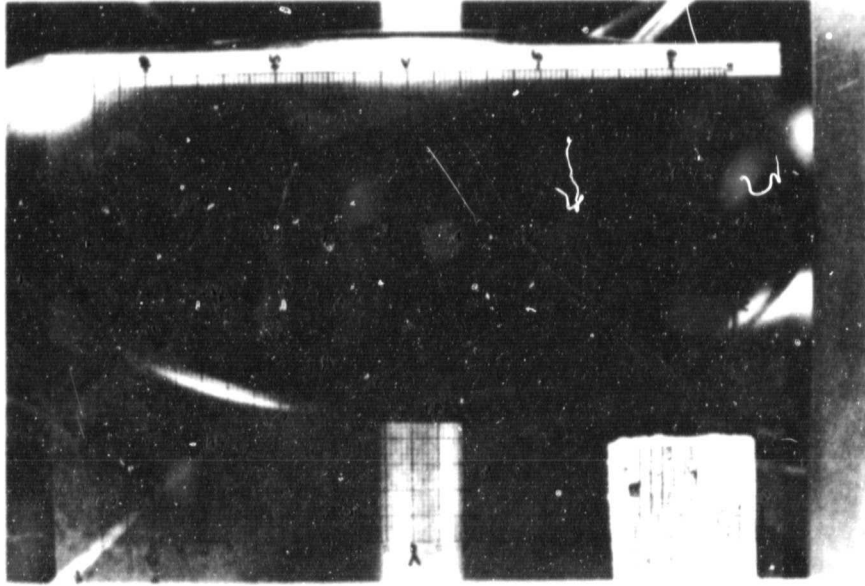
FIGURE 27. Lateral Deflection versus Lateral Load

Lateral Load = 68 N

Lateral Load = 0 N
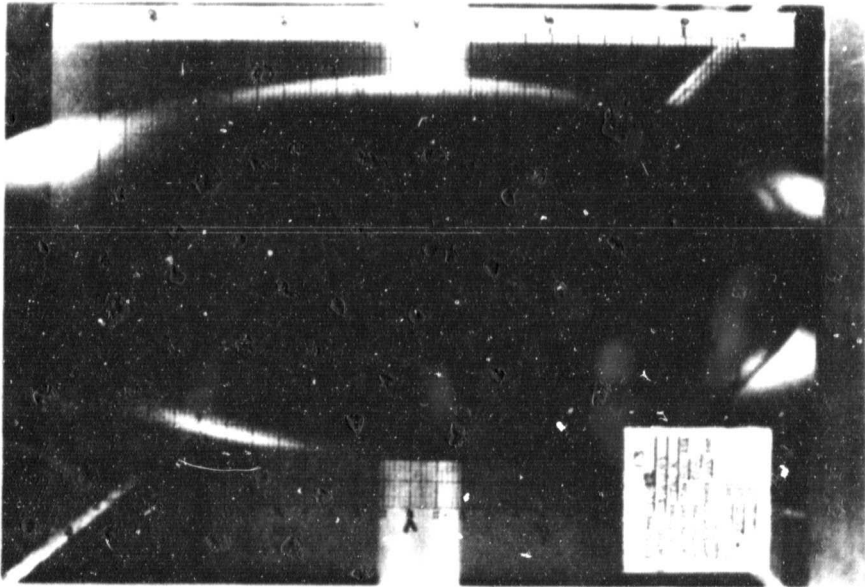
FIGURE 28. Contact Area Photographs with 114 N Normal Load

coordinate grid configuration used when both normal and lateral loads were applied. Greater grid dependency was noted in this analysis than in any of those preceding it. An iterative scheme was again used to distribute the loading at contact nodal points in the footprint area. With this type of loading, calculated results seemed to indicate a softer structure that in the previous work of Miller and Mack, where stiffness was overpredicted. In this work, computed vertical deflections were 10% to 20% greater than experimental values.

10. CONCLUSION

Over the life of this grant, four papers, seven theses, and four progress reports have been issued. These are listed below:

A. Papers

Flugrad, D. R. and Miller, B. A., "Experimental and Finite Element Study of a Standing Torus Under Normal and Tangential Loads," Proceedings, Tire Modeling Workshop, Langley Research Center, Hampton, Va., Sept. 7-9, 1982, NASA CP 2264, pp. 141-162.

Mack, M. J., Jr., Hill, D. E., and Baumgarten, J. R., "Analytical and Experimental Study of a Standing Torus with Normal Loads," Proceedings, Tire Modeling Workshop, Langley Research Center, Hampton, Va., Sept. 7-9, 1982, NASA CP 2264, pp. 123-140.

Mack, M. J., Gassman, P. M., and Baumgarten, J. R., "The Analysis of a Thin-Walled Pressurized Torus Loaded by Contact With a Plane," Proceedings, AIAA/ASME/ASCE/AHS 23rd Structures, Structural Dynamics, and Materials Conference, May 10-12, 1982, New Orleans, pp. 181-187. To be published, AIAA Journal, Oct. 1983.

Hill, D. E. and Baumgarten, J. R., "Experimental Stress Analysis of a Thin-Walled Pressurized Torus Loaded by Contact With a Plane," Proceedings, AIAA/ASME/ASCE/AHS, 23rd Structures, Structural Dynamics and Materials Conference, May 10-12, 1982, New Orleans. To be published, AIAA Journal, Nov. 1983.

B. Theses

Pau, Timothy R., "The Experimental and Finite Element Analysis of an Inflated Toroidal Structure Loaded Normally and Laterally," M.S. Thesis, Dept. of Mechanical Engineering, Iowa State University, 1983.

Bucher, Michael S., "A Study in Rim Boundary Modeling," M.S. Thesis, Dept. of Mechanical Engineering, Iowa State University, 1983.

Miller, Bruce, A., "Experimental and Finite Element Analysis of an Inflated Torus with Normal and Tangential Loading," M.S. Thesis, Dept. of Mechanical Engineering, Iowa State University, 1983.

Mack, Jr., M. J., "The Finite Element Analysis of an Inflated Toroidal Structure," M.S. Thesis, Dept. of Mechanical Engineering, Iowa State University, 1981.

Hill, D. E., "Experimental Stress Analysis of an Inflated Toroidal Structure," M.S. Thesis, Dept. of Mechanical Engineering, Iowa State University, 1981.

Gassman, P. M., "Deflection and Contact Area of a Standing Torus,"
M.S. Thesis, Dept. of Mechanical Engineering, Iowa State University,
1980.

Oguoma, O. N., "Analysis of the Contact Area of Toroidal Air Springs,"
M.S. Thesis, Dept. of Mechanical Engineering, Iowa State University,
1980.

C. Progress Reports

Mack, Jr., M. J., Hill, D. E., and Baumgarten, J. R., "Analytical
and Experimental Study of a Standing Torus with Normal Loads,"
E.R.I. Interim Report, NASA Grant NSG1605, ISU-ERI-Ames-83050,
Engineering Research Institute, Iowa State University, July 1982.

Hill, D. E. and Baumgarten, J. R., "The Experimental Stress Analysis
of a Thin-Walled Pressurized Torus Loaded by Contact with a Plane,"
E.R.I. Interim Report, NASA Grant NSG1605, ISU-ERI-Ames-81407,
Engineering Research Institute, Iowa State University, July 1981.

Mack, Jr., M. J., Gassman, P. M., and Baumgarten, J. R., "The
Analysis of a Thin-Walled Pressurized Torus Loaded by Contact with
a Plane," E.R.I. Interim Report, NASA Grant NSG1605, ISU-ERI-Ames-
81236, Engineering Research Institute, Iowa State University, May
1981.

Baumgarten, J. R., "Load Deflection Characteristics of Inflatable
Structures," Final Report, ISU-ERI-Ames-79067, NASA Grant NSG-1506,
Engineering Research Institute, Iowa State University, November 1978.

D. Papers Under Review

There are currently three papers under review for the 1984 AIAA/ASME
Structures Conference which have been abstracted from the work of
Pau, Bucher, Miller, Flugrad, and Baumgarten.

BIBLIOGRAPHY

1. Orley, J. F., "Control of Punch Press Noise Generation Through Variable Resilient Mounting," M.S. Thesis, University of Nebraska, 1975.

2. Baumgarten, J. R. and Orley, J. E., "Noise and Vibration Isolation Using Air Springs," Proceedings 1978 International Conference on Noise Control Engineering, San Francisco, May 8-10, 1978, pp. 1033-1035.

3. Andersen, G. E., "Prediction of the Natural Vibration Frequency for a Torus Shaped Air Spring and Mass System," M.S. Thesis, University of Nebraska, 1975.

4. Baumgarten, J. R. and Andersen, G. E., "Analysis of Airspring Isolators," Proceedings of the 5th World Congress on ToMM, Vol. 1, Montreal, Canada, July 1, 1979, pp. 337-340.

5. Chomos, S. E., "Prediction of the Load-Deflection Characteristics of a Toroidal Air-Rubber Spring," M.S. Thesis, University of Nebraska, 1979.

6. Oguoma, O. N., "Analysis of the Contact Area of Toroidal Air Springs," M.S. Thesis, Dept. of Mechanical Engineering, Iowa State University, 1980.

7. Gassman, P. M., "Deflection and Contact Area of a Standing Torus," M.S. Thesis, Dept. of Mechanical Engineering, Iowa State University, 1980.

8. Mack, Jr., M. J., "The Finite Element Analysis of an Inflated Toroidal Structure," M.S. Thesis, Dept. of Mechanical Engineering, Iowa State University, 1981.

9. Hill, D. E., "Experimental Stress Analysis of an Inflated Toroidal Structure," M.S. Thesis, Dept. of Mechanical Engineering, Iowa State University, 1981.

10. Miller, B. A., "Experimental and Finite Element Analysis of an Inflated Torous with Normal and Tangential Loading," M.S. Thesis, Dept. of Mechanical Engineering, Iowa State University, 1983.

11. Bucher, M. S., "A Study in Rim Boundary Modeling," M.S. Thesis, Dept. of Mechanical Engineering, Iowa State University, 1983.

12. Pau, T. R., "The Experimental and Finite Element Analysis of an Inflated Toroidal Structure Loaded Normally and Laterally," M.S. Thesis, Dept. of Mechanical Engineering, Iowa State University, 1983.